ANL-ART-199

Initial development of a method for correlating indentation test results to damage accumulation in high temperature structural materials

Applied Materials Division

ANL-ART-199

Initial development of a method for correlating indentation test results to damage accumulation in high temperature structural materials

---

Applied Materials Division
Argonne National Laboratory

August 2020

Prepared by

Aritra Chakraborty, Argonne National Laboratory
M. C. Messner, Argonne National Laboratory
T.-L. Sham, Argonne National Laboratory

Abstract

This report describes an experimental approach based on microindentation creep or relaxation tests for assessing the remaining creep life of a sample material. The objective for this experimental program is to complement the development of passively loaded in situ surveillance specimens. These surveillance specimens could be placed in future advanced reactors to assess the degradation of structural properties, primary creep and creep-fatigue life, when the material is exposed to actual reactor operating conditions. The specimens and the corresponding indentation test protocol could form the basis of a structural health monitoring program designed to ensure the safe continued operation of the component given the relatively unknown effect of the reactor coolant chemistry, radiation exposure, and other environmental effects on the material properties of the constituent structural materials.

Table of Contents

List of Figures

List of Tables

1 Introduction

1.1 In-situ surveillance specimens

Future advanced reactors will experience harsh service environments, including long times spent at high temperatures, exposed to corrosive coolants and potentially high radiation doses [1, 2]. The long-term reliability of candidate structural materials under these conditions is largely unknown.

An in situ surveillance program is one possible approach for verifying the structural integrity of reactor components under actual service conditions. Monitoring specimens could be inserted into reactor components at key locations and periodically monitored to ensure the component retains adequate structural strength. The monitoring specimens would be manufactured from the same material and using similar manufacturing processes as the component itself. The specimens would be positioned to experience representative service conditions. Specimens would then be removed periodically and tested to ensure the component retains the required strength.

Two potential models are possible for surveillance programs:

1. A verification program where periodic measurement of the mechanical properties of the test articles ensures the component retains sufficient structural integrity. This type of program exposes the test specimens to representative service conditions.

2. A canary program where the test articles directly guard against the premature failure of the component. Here specimen service conditions and loading must exceed the actual component conditions so that the test articles fail before the corresponding structural component.

With either mode of monitoring program the specimen data could also be used to justify future life extensions.

The existing LWR fleet maintains surveillance programs, specifically applying the verification model. For example, PWRs operate a toughness surveillance program using standardized specimens to guard against radiation-induced embrittlement of the vessel steel [3]. Some constraints on the test specimen and the type of testing required by the program are common between current LWRs and future advanced reactors. For example, specimens will need to be sized to fit in reactor components with minimal disruption to the component operation. Testing will likely need to occur in a hot cell, which again limits the geometry of the specimen as well as the types of tests available.

However, there are several aspects in designing a surveillance specimen unique to advanced high temperature reactors. For example, the primary modes of structural degradation in high temperature components, creep and creep-fatigue damage, are related to the component temperature, service time, and mechanical load. The first two factors are easy to replicate with a surveillance specimen, but the third requires a specimen that can be mechanically loaded in situ. Test reactors, for example the Halden research reactor [4], have the ability to actively load a specimen to the reactor operating conditions. Such systems typically rely on hydraulic rabbits to deliver and retrieve the test rig. These systems will be unavailable in operating commercial reactors and so passively loaded specimens may be required. These specimens induce a mechanical load in the specimen using the ambient reactor

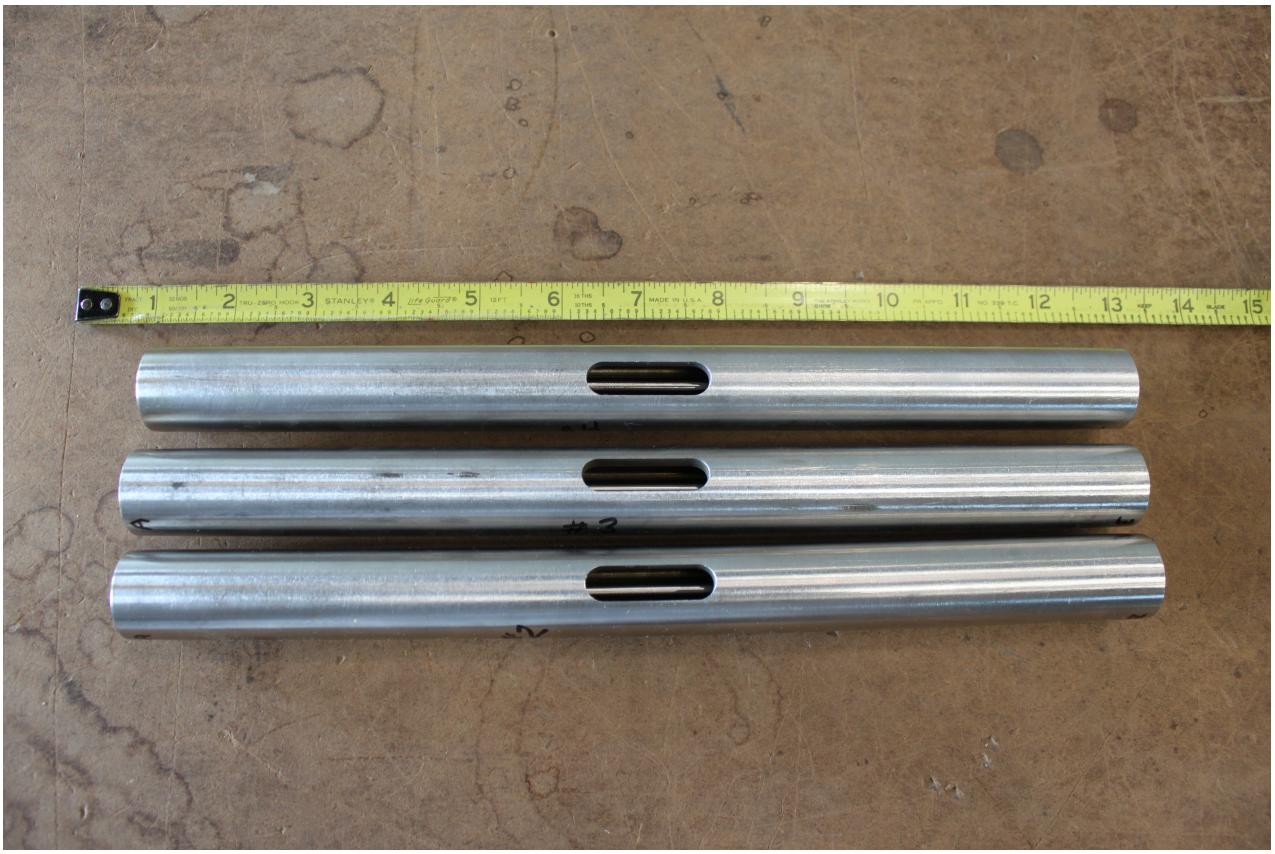

Figure 1.1: Oversized test specimen developed at Argonne National Laboratory designed to demonstrate the concept of a passively loaded test article.

conditions. An example might be a specimen loaded through a mismatch in material coefficient of thermal expansion, meaning an increase or decrease in the component temperature induces a mechanical load in the test article [5]. Argonne National Laboratory is developing passively loaded mechanical surveillance specimens to assess creep-fatigue strength (see Fig. 1.1). A parallel report will report progress on this development program.

Time dependent properties are another challenge unique to high temperature systems. Unlike lower temperature systems like LWRs the mechanical properties controlling the structural life of a component in a high temperature reactor are time dependent. For example, creep strength can only be assessed as a function of temperature and time. This means that there is no obvious quick test can that be used to assess critical material properties.

Assuming the test specimen can deliver representative (verification program) or suitable bounding (canary program) temperatures, radiation doses, coolant exposure, and mechanical loading relative to the actual component, the corresponding testing program must determine the *remaining life* of the test specimens. The remaining life is the time the specimen can maintain mechanical integrity assuming it remains loaded at fixed conditions. An example might be an interrupted creep test. If, under some combination of temperature and stress, a specimen has a rupture life of 100,000 hours but the specimen was removed from the creep frame at 25,000 hours the remaining life of the specimen would be 75,000 hours. Determining the remaining life of the in situ surveillance specimens is a key step in a monitoring program.

This report addresses the challenge of developing a relatively short term test, compatible with the constraints on the test specimen geometry described above, that can assess the remaining life of a test article. This type of testing methodology will be a key aspect of a practical in situ monitoring program in future advanced reactors.

1.2 Predicting remaining life

The objective of any test program would be to predict the remaining life of the test articles, assuming they will continue to be loaded under the same conditions in the future. The program must rely on periodic, intermittent testing. For example, some number of surveillance articles could be examined every plant maintenance outage. As described above, the reactor conditions will impose limits of the types of tests. The specimens are likely to remain radioactive for some amount of time after being removed from the component and so any test must accommodate relatively small specimens, to reduce cool down time, and may need to be completed in a hot cell environment.

Remaining life prediction for high temperature components is one aspect of a fitness for service analysis. Fitness for service analysis presumes an operating plant and so there are few if any guidelines for assessing high temperature nuclear components. However, in the U.S., the ASME-FFS-1/API-579 standard [6] provides guidance that, while focused on petrochemical components, could be applied to other high temperature systems. The general approach described in the standard is to first characterize the component and relevant operating conditions, often focusing on a discrete flaw, and then determine a list of plausible failure mechanisms. The standard provides guidance for assessing the remaining life of the component against a variety of these potential failure modes.

Part 10 of the standard applies to temperatures operating in the creep range. It includes method for assessing the remaining life of the component considering creep rupture and creep-fatigue interaction. The detailed procedure uses a damage parameter based on the MPC Omega [7] method. A damage parameter is a variable typically ranging from 0 to 1 with 0 describing virgin material and 1 denoting failed material. The MPC Omega model provides a tool for assessing the current and future values of this parameter given material properties and the component operating conditions. This approach assumes

- The past operating conditions can be used to compute the current damage fraction.
- The material properties, in particular the creep rate which the Omega model ties to damage accumulation, are fully known and not affected by the component service environment.

The British R5 standard provides a similar approach. These methods require a description of the in-service creep and creep-fatigue performance of the material and are therefore more suitable to operating systems with extensive service history (which can be used to develop and calibrate models accounting for environmental conditions). This general approach is not suitable for a monitoring program on a new advanced reactor system, where the effect of the environment on the material may be substantially unknown.

An approach tying the remaining life of the material to the prior service conditions though experimental data will be required for an in situ surveillance program in new, advanced

reactor systems. This report describes the theory of a such a testing program assessing the remaining life of surveillance specimens using microindentation stress relaxation and creep experiments. This approach fulfills the basic criteria outlined above:

1. It assesses the remaining life of the articles using experimental measurements of their current material properties. As such the approach can account for the unknown degradation caused by the component service environment.

2. Microindentation tests require relatively small volumes of material meaning the test articles can be small enough to not interfere with the component operation.

3. Similarly, for small specimens the indentation tests can be performed in a hot cell environment.

4. The tests are non-destructive. This means that test articles can be tested and then returned to the component service conditions at the conclusion of the maintenance outage. This reduces the number of test articles required, as they can be reused, rather than expending one or more articles per outage. Reuse could reduce the impact of the test articles on the component operation.

1.3 Outline

Chapter 2 of the report describes the theory of an indentation testing program for predicting the remaining life of a material with an unknown prior service history. This theory is developed with finite element simulations of indentation experiments using known constitutive models. This approach, where the actual remaining life of the material is known in advance, allows for theoretical verification of the approach. However, the method can be applied to predicting the remaining life of a material with an unknown past service history, assuming a relatively limited set of properties are known for virgin material. Chapter 3 then describes a step by step experimental procedure.

This report focuses on a subset of the complete problem — failure under steady-state loading conditions. In actuality reactor components will be affected by creep-fatigue interaction requiring an experimental method for predicting remaining life under cyclic loading. The method described here is a valuable first step, both in that it provides a plausible approach for relevant service conditions and because, for some advanced reactor concepts, fatigue damage and creep-fatigue interaction may be negligible in the actual operating conditions.

2 Determining remaining life from indentation tests

Indentation relaxation experiments have been used to identify uniaxial creep parameters, especially when considering isotropic materials and without significant primary creep (hardening) regimes. In this chapter, we describe a methodology to estimate the remaining life of a material using indentation relaxation tests, by identifying the power law creep parameters. The methodology is illustrated using synthetic experiments, i.e., data generated using finite element simulations of indentation experiments.

2.1 Simulation details

2.1.1 Indentation model

Figure 2.1 shows a typical indentation schematic with a spherical indenter with an indentation load P. It is evident from the schematic that the actual depth of the substrate, h_s, is different from the contact depth of the indenter, h_i. The contact radius, a_c can be obtained when h_i is known. However, measurement of h_i is not possible via the indentation equipment and can only be obtained post indentation, while a_c is obtained using h_s which results directly from the indentation load–displacement curve. The corresponding indentation finite element (FE) simulation is performed using the contact module of the open source package Multiphysics Object Oriented Simulation Environment (MOOSE) [8], while the material models for the indenter and the substrate are provided using the Nuclear Engineering Material Library (NEML) (https://github.com/Argonne-National-Laboratory/neml), also coupled with MOOSE. The 2D axisymmetric mesh and the geometry is shown in Fig. 2.2. The substrate radius is four times the indenter radius and the substrate depth is much larger than the indentation depth. The region close to the indenter is meshed finer to accommodate large deformations. For contact, the rigid indenter acts as the master while the substrate acts as the slave. Displacement of the substrate bottom is fixed to zero to avoid rigid body translation. Using this geometry, we perform an initial elastic FE simulation and compare the numerical indentation load-depth result to that of an analytical solution obtained using elastic Hertz contact. The material properties for the indenter and the substrate is listed in

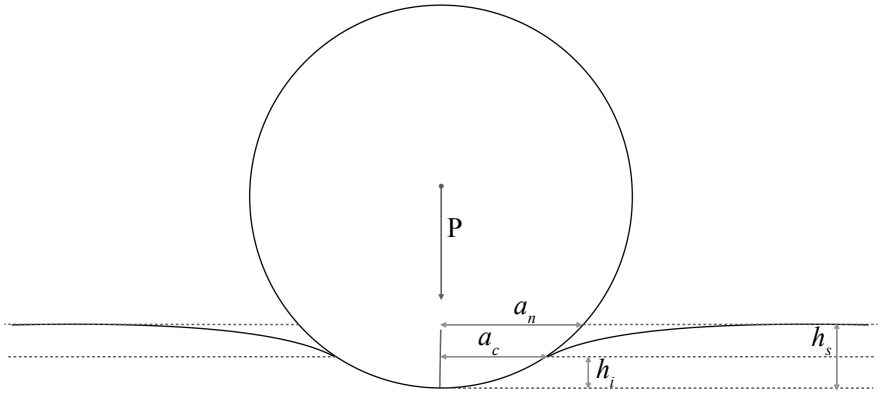

Figure 2.1: Schematic showing indentation simulation. h_i and h_s refer to the actual indenter displacement and the net substrate displacement (nominal displacement) respectively. a_c and a_n are the actual and nominal contact radius calculated from h_i and h_s respectively.

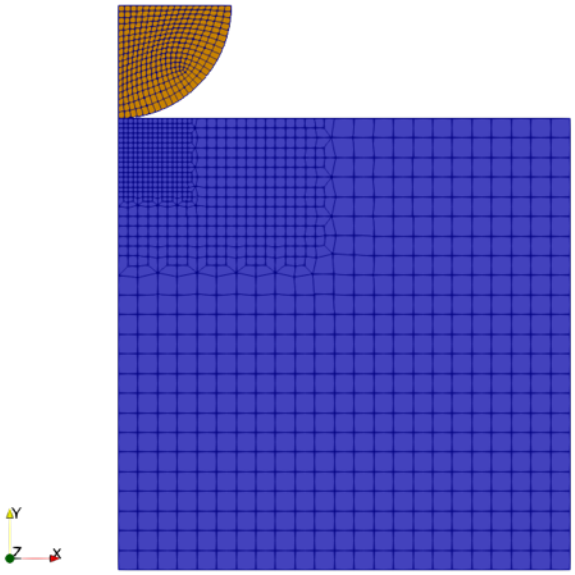

Figure 2.2: Geometry for the FE simulation.

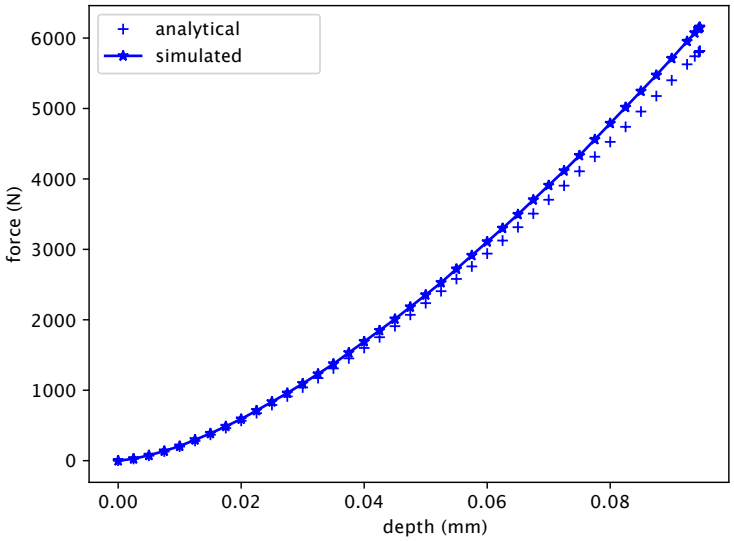

Figure 2.3: Comparison between numerical and analytical solution.

Table 2.1: Parameters for the elastic simulation mimicking Hertz contact.

parameter	**indenter**	**substrate**
Young's modulus	1500 GPa	150 GPa
Poisson's ratio	0.2	0.31

Table 2.1. The indentation load, P, is calculated by integrating the nodal (reaction) forces on the top surface of the indenter, while the displacement is the vertical displacement of the nodes on the top surface. The results show a close similarity between the numerical and analytical solutions, see Fig. 2.3. Subsequently, we use this FE geometry and perform indentation creep simulations using an inelastic material model.

2.1.2 Inelastic model

The one dimensional inelastic material model used for the indentation simulations is based on small strain deformation theory where the total strain rate is sum of the elastic and creep strain rate components:

$$\dot{\epsilon} = \dot{\epsilon}_e + \dot{\epsilon}_c \tag{2.1}$$

with the elastic strain rate following Hooke's law, which for uniaxial condition is,

$$\dot{\epsilon}_e = E : \dot{\sigma} \tag{2.2}$$

The creep rate is assumed to follow the Norton–Bailey power law relationship,

$$\dot{\epsilon}_c = A_c \left(\frac{\sigma}{1-\omega} \right)^{n_c} \tag{2.3}$$

where, ω is the damage variable. A_c and n_c are the creep parameters. The damage rate is assumed to follow the classical model by [9], given by:

$$\dot{\omega} = \left(\frac{\sigma}{A_d} \right)^{\zeta} (1-\omega)^{-\phi} \tag{2.4}$$

where A_d, ϕ and ζ are the damage parameters. The five adjustable parameters of the model (2 creep and 3 damage) depend on temperature and deformation history of the material. In this work we generate synthetic creep data for certain combination of these parameters (representing different temperature and/or deformation history) and try to recover the instantaneous creep rates from the corresponding indentation simulation. The damage parameter values are fixed to $A_d = 1000.0$, $\zeta = 3.5$, and $\phi = 2.0$, respectively unless otherwise mentioned. Using synthetic data for the present analysis avoids the artifacts associated with experimental data acquisition.

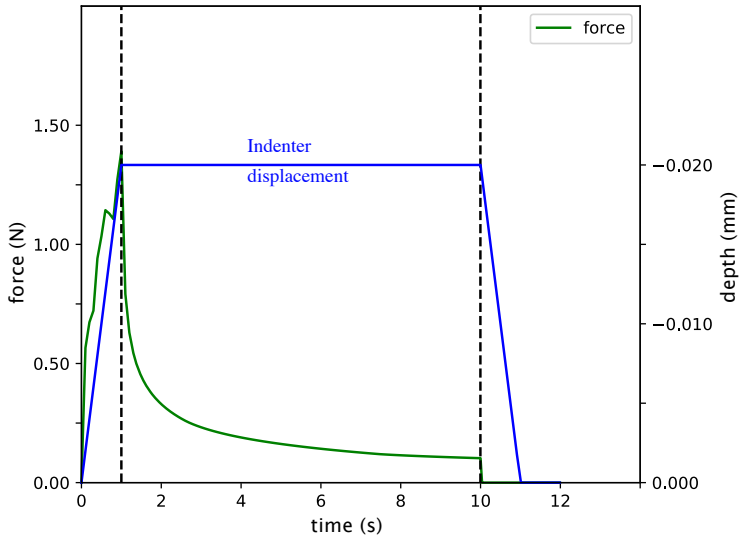

Figure 2.4: Typical indentation output curve.

2.2 Indentation creep

This work simulates two types of indentation creep experiments with FE simulations: constant indent depth hold and constant indent load hold. The blue curve in Fig. 2.4 shows a typical indenter response during constant depth relaxation experiments. In this experimental condition the indenter is displaced into the sample to a certain depth (0.02 mm in this study) and then kept constant. The stresses generated due to indentation relaxes by creep during the hold period as reflected by the force displacement curve, green line in Fig. 2.4. The region of concern in this study is the indenter response during this hold period, and the objective is to recover the creep parameters (n_c and A_c) from the relaxation data. The expression of indentation creep, ϵ_i, for geometrically self similar indenter (cone or sphere) without considering and history dependence, is given as, [10]:

$$\dot{\epsilon}_i = \frac{\dot{h}_i}{h_i} = \beta\, p_m^N, \tag{2.5}$$

where β and N are creep parameters, and p_m is the actual contact pressure defined as indentation load (P) / Actual contact area (πa_c^2). h_i refers to the actual indentation depth as labelled in Fig. 2.1. Based on several investigations, it is found that the creep exponent is same for both indentation and uniaxial creep tests, $N = n_c$, which will also be verified later in the report. The generalized indentation creep rate proposed by Bower et al. [11] relating uniaxial and indentation creep is then given as,

$$\dot{\epsilon}_i = A_c \left(p_m/F\right)^{n_c}, \tag{2.6}$$

where F is the "dimensionless contact pressure", and A_c and n_c are the uniaxial creep parameters. Additionally, since it is difficult to measure the true contact area from the indentation experiments, actual contact pressure can be replaced by the nominal contact

pressure (p_{nom}) based on the nominal contact area (πa_n^2) [12]. Using the above notation the indentation creep can be written as,

$$\dot{\epsilon}_i = \frac{A_c}{F_c^n c^{2n_c}} (p_{nom})^{n_c}, \tag{2.7}$$

where c is the "pile-up/sink-in" parameter and is the ratio of the actual contact area to nominal contact area (a_c/a_n). Comparing to the power law indentation creep equation, the relation between indentation creep parameters (β and N) with uniaxial creep parameters (A_c and n_c) is,

$$N = n_c \tag{2.8}$$

$$\beta = \frac{A_c}{F^n c^{2n}} \tag{2.9}$$

The values of the F and c depend on the stress exponent N and have been tabulated by Bower et al. [11] through finite element simulations.

2.3 Synthetic indentation creep and parameter extraction

In this section we perform finite element simulations of indentation creep and compare the obtained creep parameters to an equivalent uniaxial creep simulation. The advantage of using such synthetic experiments for comparison is the a priori knowledge of the parameter values, thus enabling quantifiable error estimation [13, 14]. Moreover, the relationship between the indentation and uniaxial creep coefficients is also modified from its original form, see Eq. (2.8),

$$\beta = \frac{A_c}{(F\kappa)^n c^{2n}} \tag{2.10}$$

where κ is fitted by comparing simulations of the creep indentation to the actual, known power law creep parameters of the simulated material.

With this, a series of constant depth hold (see Fig. 2.1) indentation creep finite element simulations are performed for different material parameters (n_c and A_c) using the mesh shown in Fig. 2.2. The creep parameters from the load relaxation regime is obtained by fitting the indentation stress rate and indentation stress into the creep power law relation, based on the following,

$$\dot{\epsilon} = \dot{\epsilon}_e + \dot{\epsilon}_i, \tag{2.11}$$

where the total strain rate $\dot{\epsilon}$ is the sum of the elastic ($\dot{\epsilon}_e$) and the indentation creep strain rate ($\dot{\epsilon}_i$). During constant indentation depth hold test the total strain is constant, leading to,

$$\dot{\epsilon}_e = -\dot{\epsilon}_i, \tag{2.12}$$

$$\frac{\dot{\sigma}}{E_{eff}} = -\dot{\epsilon}_i, \tag{2.13}$$

Table 2.2: Comparison of creep parameters obtained from indentation to that of uniaxial.

Uniaxial		Indentation		
n_c	A_c	N	β, (κ)	β_0
4.0	2×10^{-11}	3.97	3.3×10^{-11}, (1.665)	4.4×10^{-12}
5.0	2×10^{-11}	4.87	3.6×10^{-11}, (1.615)	3.5×10^{-12}
6.0	2×10^{-11}	5.80	4.0×10^{-11}, (1.565)	3.0×10^{-12}
8.0	2×10^{-11}	7.70	3.5×10^{-11}, (1.465)	1.8×10^{-12}
10.0	2×10^{-11}	9.71	3.3×10^{-11}, (1.42)	1.1×10^{-12}
12.0	2×10^{-13}	11.60	4.0×10^{-13}, (1.38)	9.5×10^{-15}
14.0	2×10^{-13}	13.10	1.6×10^{-13}, (1.34)	3.4×10^{-15}
16.0	2×10^{-15}	15.10	1.0×10^{-15}, (1.30)	2.0×10^{-17}

with, σ and E_{eff} being the indentation stress and the effective Young's modulus respectively,

$$\sigma = \frac{P}{A_{nom}}, \tag{2.14}$$

$$\frac{1}{E_{eff}} = \frac{1-\nu_i^2}{E_{indenter}} + \frac{1-\nu_s^2}{E_{substrate}}, \tag{2.15}$$

where, P is the indentation load, A_{nom} is the nominal contact area defined earlier, and $E_{indenter}$ and $E_{substrate}$ being the Young's modulus of the indenter and the substrate respectively. ν_i and ν_s are the Poisson's ratio of the indenter and the substrate respectively. Using the indentation creep power law relation, the creep parameters (β and N) can be obtained by fitting the stress rate and stress,

$$\frac{\dot{\sigma}}{E_{eff}} = -\dot{\epsilon}_i = -\beta\sigma^N \tag{2.16}$$

Table 2.2 lists the creep parameters from the various indentation creep (synthetic) experiments along with their reference values (uniaxial counterparts). The difference between the creep coefficient (β) values obtained using the modified relation Eq. (2.10) to the original form (β_0) mentioned in Eq. (2.8) is also shown in the columns 4 and 5 respectively with the used values of κ in parenthesis. The scale factor (κ) was selected to best match the reference solution and our finite element analysis. Clearly the stress exponents between the indentation and uniaxial tests are the almost the same, while the creep coefficients are recovered within the correct order of magnitude. However, using the original relationship by Bower et al. [11] the creep coefficients seemed to vary by at least an order of magnitude.

We also investigate whether the calibrated κ values change with a different material (i.e., for different Young's modulus and creep coefficient A_c) or for a different mesh.

2.3.1 Effect of Young's modulus

The methodology outlined above to extract creep parameters from constant depth hold indentation creep is repeated for a material with different Young's modulus (of 15 and

70 GPa) and at different stress exponents.

Table 2.3: Comparison of creep parameters at E = 15 GPa and $\nu = 0.31$.

Uniaxial		Indentation		
n_c	A_c	N	β, (κ)	β_0
4.0	2×10^{-11}	4.50	1.4×10^{-11}, (1.665)	1.4×10^{-12}
6.0	2×10^{-11}	5.85	5.9×10^{-11}, (1.565)	4.3×10^{-12}
8.0	2×10^{-11}	7.61	6.5×10^{-11}, (1.465)	3.6×10^{-12}
10.0	2×10^{-11}	9.40	7.9×10^{-11}, (1.42)	3.0×10^{-12}

Table 2.4: Comparison of creep parameters at E = 70 GPa and $\nu = 0.31$.

Uniaxial		Indentation		
n_c	A_c	N	β, (κ)	β_0
4.0	2×10^{-11}	4.14	1.9×10^{-11}, (1.665)	2.3×10^{-12}
6.0	2×10^{-11}	5.84	3.9×10^{-11}, (1.565)	2.8×10^{-12}
8.0	2×10^{-11}	7.65	4.5×10^{-11}, (1.465)	2.4×10^{-12}
10.0	2×10^{-11}	9.56	4.5×10^{-11}, (1.42)	1.6×10^{-12}

Tables 2.3 and 2.4 compares the creep parameters from indentation creep curves to that of their actual values for two different substrate Young's modulus of 15 and 70 GPa. Also shown are the differences in the creep coefficients using the modified equation versus the one proposed in [11]. Clearly, using the same κ values as before, the obtained creep coefficients are within the same order of magnitude of the actual values, suggesting that κ values does not change with the material's modulus.

2.3.2 Effect of creep coefficient

We also investigate whether the κ values depend on the creep coefficient of the material, by repeating the parameter extraction method for materials with different creep coefficients and at different stress exponents. The results highlighted in Table 2.5 indicate the κ values work well for different creep coefficients as the extracted parameters are within the same order of magnitude.

2.3.3 Effect of mesh quality

A reason for non unity κ values (i.e., deviating from Bower's solution) can also be due to the numerical derivatives and data extraction errors, which generally reduce with finer mesh quality. To see how mesh refinement affect these κ values established previously, the constant depth hold indentation simulation is repeated with a finer mesh, Fig. 2.5, at different stress

Table 2.5: Effect of creep coefficient.

Uniaxial		Indentation		
n_c	A_c	N	β, (κ)	β_0
4.0	2×10^{-9}	3.94	2.5×10^{-9}, (1.665)	3.4×10^{-10}
6.0	2×10^{-9}	5.80	3.4×10^{-9}, (1.565)	2.6×10^{-10}
7.0	2×10^{-9}	6.90	2.7×10^{-9}, (1.515)	1.5×10^{-10}
4.0	2×10^{-13}	4.20	2.1×10^{-13}, (1.665)	2.5×10^{-14}
6.0	2×10^{-13}	5.94	2.1×10^{-13}, (1.565)	2.1×10^{-14}
8.0	2×10^{-13}	7.72	4.5×10^{-13}, (1.465)	2.4×10^{-14}

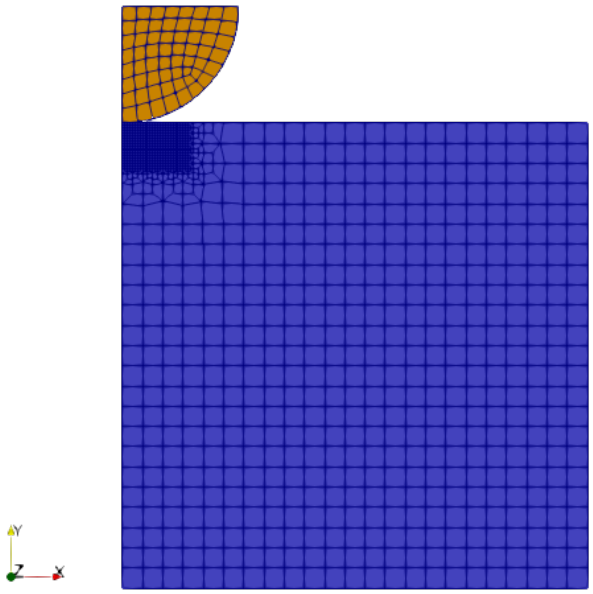

Figure 2.5: Finer FE mesh.

exponents. Table 2.6 shows the extracted creep parameters using the same κ values as established earlier but with a finer mesh. It seems that these values are indeed independent of mesh quality for the present case as the previous results are consistent even with a finer mesh.

Apart from the constant depth hold tests, we also performed constant load hold indentation creep simulations, and compare the extracted parameters to the exact counterparts.

Table 2.6: Creep parameters obtained for a finer mesh with consistent κ values.

Uniaxial		Indentation		
n_c	A_c	N	β, (κ)	β_0
4.0	2×10^{-11}	3.95	3.3×10^{-11}, (1.665)	4.4×10^{-12}
6.0	2×10^{-11}	5.98	2.2×10^{-11}, (1.565)	1.5×10^{-12}
8.0	2×10^{-11}	7.85	2.0×10^{-11}, (1.465)	1.0×10^{-12}
10.0	2×10^{-11}	9.78	2.0×10^{-11}, (1.42)	6.6×10^{-13}

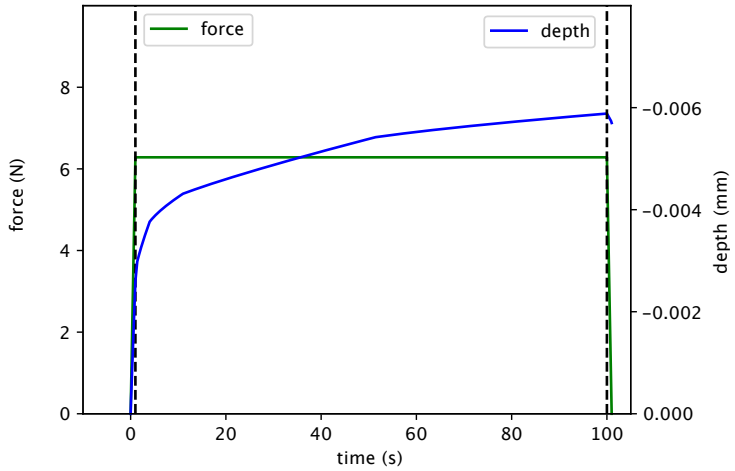

Figure 2.6: Constant load hold indentation boundary condition.

2.4 Constant load hold tests

In constant load hold indentation creep tests the load in the indenter remains constant while the contact area changes to relax the stresses, Fig. 2.6. A longer hold period is set for constant load hold tests, to ensure sufficient points in the steady state creep regime. We obtain the creep parameters by fitting the indentation strain rate and the indentation stress to the power law relationship,

$$\dot{\epsilon}_i = \dot{h}_s/h_s = \beta p_m^N, \tag{2.17}$$

$$p_m = P/\pi a_n^2 \tag{2.18}$$

where h_s, P, a_n, are the substrate depth, indentation load, and nominal radius during the hold period, see Fig. 2.1. Moreover, mostly the tail end of the relaxation curve is used for the analysis thus neglecting the primary creep regime [15]. The test is performed for different stress exponents and creep coefficients and the creep coefficients obtained with Bower's method seem to suffice (Table 2.7). It is crucial to note that for constant load hold tests, the results are more sensitive to the data as the creep rates are obtained using numerical derivatives. Depending on the fidelity of the data, the scatter in the results can vary a couple of orders of magnitude in the creep coefficient, thus proper data filtering is

Table 2.7: Constant hold tests

Uniaxial		Indentation	
n_c	A_c	N	β_0
4.0	2×10^{-14}	4.91	2.7×10^{-14}
6.0	2×10^{-14}	6.01	3.2×10^{-14}
8.0	2×10^{-16}	7.99	1.2×10^{-16}
10.0	2×10^{-20}	9.72	1.2×10^{-20}

crucial, especially when using real experimental data. Since, in this work we know the creep parameters, we truncate the data of creep rate and indentation stress such that the stress exponent is closest to the actual value. For real experiments, this might not be feasible, hence the analysis should be repeated with different truncations of the data to estimate how the exponent value changes.

2.5 Indentation tests on pre-damaged material

In this section we perform the creep parameter extraction methodology for a damaged material, which for the present case of synthetic experiments corresponds to starting the indentation FE simulation with an initial history. This analysis is repeated with different initial history values, akin to studying different damaged material, and the instantaneous creep rates obtained using the extracted creep parameters are compared to actual uniaxial creep rates. If the two creep rates are close, then the present procedure of estimating remaining material life using indentation creep is feasible.

As an example we show the results for a material with creep parameters $n_c = 6.0$ and $A_c = 2 \times 10^{-16}$, where we extract creep parameters using indentation at different times during the test (i.e., different initial damage) and compare the instantaneous creep rates with their corresponding uniaxial values. The uniaxial creep stress is selected as 100 MPa, while the maximum indentation depth is fixed to 0.04 mm. As expected the stress exponents do not change with different damaged state of the material, while the extracted creep coefficient does change. Also, the κ values obtained previously are used to extract the creep coefficient. The instantaneous creep rates, $\dot{\epsilon}_i$, are obtained using the creep parameters obtained from the indentation and the creep stress, $\dot{\epsilon}_i = \beta\ (100.0)^N$, where 100 MPa is the creep stress, and are relatively close to their actual creep rates, $\dot{\epsilon}_c = A_c\ (\frac{100.0}{1-damage})^{n_c}$. Figure 2.7 compares these instantaneous creep rates for the selected material parameter against the macroscopic equivalents, along with the creep rate curve. Clearly, the creep rate values obtained from the indentation methodology matches closely with their macroscopic uniaxial values.

We repeat this methodology for different values of stress exponent and creep coefficient to test its reliability and similar results are obtained, Fig. 2.8.

As an example, consider a study with constant load hold indentation creep boundary conditions with material parameters $n_c = 6.0$, and $A_c = 2 \times 10^{-16}$. A longer hold time (400 seconds) is used for constant hold indentation creep, and the extracted creep parameters

Table 2.8: Extracted parameters and creep rates at different times for a material with creep parameters $n_c = 6.0$, and $A_c = 2 \times 10^{-16}$

time	*damage*	N	β, (κ)	$\dot{\epsilon}_i$	$\dot{\epsilon}_c$
10.0	0.0104	5.99	3.4×10^{-16}, (1.565)	0.00033	0.00021
210.0	0.0784	6.02	4.2×10^{-16}, (1.565)	0.00046	0.00033
410.0	0.1549	5.99	7.6×10^{-16}, (1.565)	0.00073	0.00055
610.0	0.2435	6.08	8.7×10^{-16}, (1.565)	0.00126	0.00106
710.0	0.2945	5.99	1.8×10^{-15}, (1.565)	0.00180	0.00162
810.0	0.3516	6.08	1.8×10^{-15}, (1.565)	0.00278	0.00269
880.0	0.4036	6.00	4.2×10^{-15}, (1.565)	0.00421	0.00444

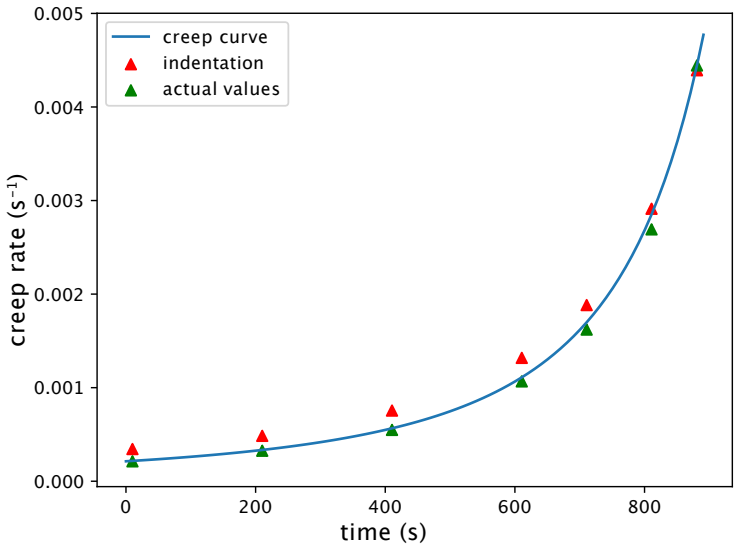

Figure 2.7: Comparing instantaneous rates as obtained from indentation to that of the corresponding macroscopic values for $n_c = 6.0$ and $A_c = 2 \times 10^{-16}$.

are shown in Table 2.9. Clearly, the parameters obtained using the constant load hold indentation creep condition is associated with a much higher error, also see Fig. 2.9. The large errors might be attributed to the numerical derivatives with respect to the indenter displacement performed to calculate the indentation creep rate.

2.6 Estimation of remaining times from extracted creep parameters

Based on the previous analysis we find that the macroscopic instantaneous creep rates can be recovered from indentation creep rates, especially with constant depth hold tests. This

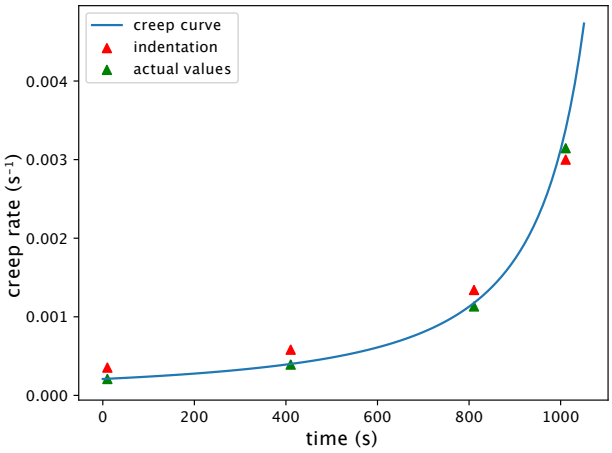

(a) $n_c = 4.0$ and $A_c = 2 \times 10^{-12}$

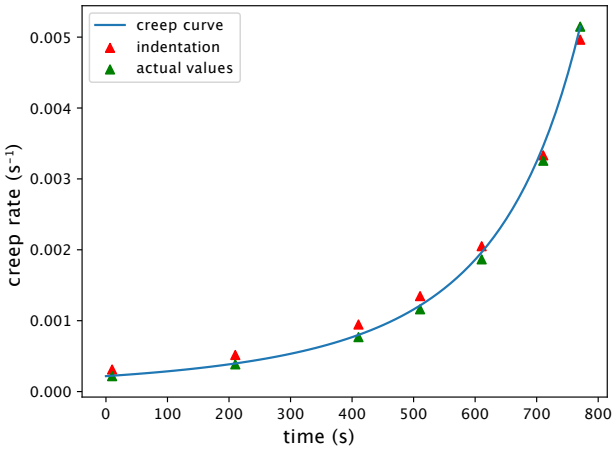

(b) $n_c = 4.0$ and $A_c = 2 \times 10^{-20}$

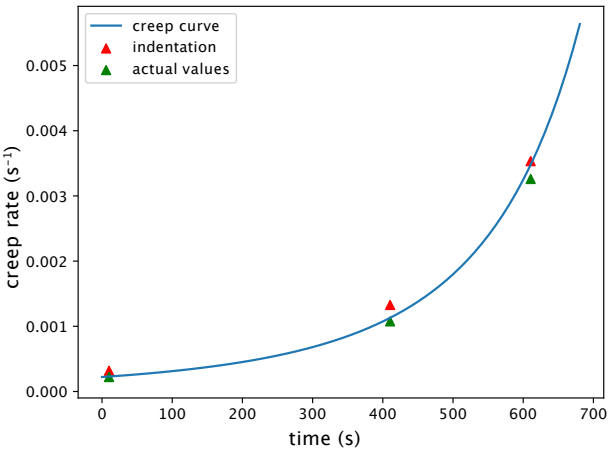

(c) $n_c = 4.0$ and $A_c = 2 \times 10^{-24}$

Figure 2.8: Comparing instantaneous creep rates extracted from constant depth hold indentation test to their corresponding macroscopic uniaxial test values at different values of n_c and A_c.

Table 2.9: Extracted parameters and creep rates for constant hold indentation creep test, at different times for a material with creep parameters $n_c = 6.0$, and $A_c = 2 \times 10^{-16}$

time	*damage*	N	β_0	$\dot{\epsilon}_i$	$\dot{\epsilon}_c$
110.0	0.0435	6.98	1.3×10^{-17}	0.001221	0.00026
410.0	0.1549	7.33	5.7×10^{-18}	0.002667	0.00055
710.0	0.2945	6.42	6.1×10^{-16}	0.004380	0.00162

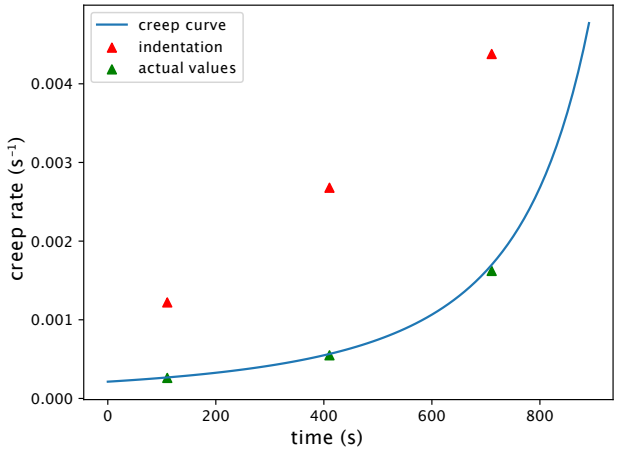

Figure 2.9: Comparison of instantaneous creep rates for constant load hold indentation creep for $n_c = 6.0$ and $A_c = 2 \times 10^{-16}$.

leads to,

$$\dot{\epsilon}_c = \dot{\epsilon}_i, \quad \text{or,} \tag{2.19}$$

$$A_c \left(\frac{\sigma}{1-\omega} \right)^{n_c} = \beta \sigma^N, \quad \text{also,} \tag{2.20}$$

$$n_c = N \tag{2.21}$$

from which the accumulated damage, ω, can be calculated as,

$$\omega = \left(1 - \frac{\beta}{A_c} \right)^{1/N} \tag{2.22}$$

Using the accumulated damage, ω, the used life can be calculated from the integrated damage evolution equation, Eq. (2.4),

$$t = \frac{1 - (1-\omega)^{\phi+1}}{(\phi+1)\left(\frac{\sigma}{A_d}\right)^{\zeta}} \tag{2.23}$$

Thus, the remaining life of damaged sample is then given by,

$$\text{remaining life} = 1 - t/t_R, \tag{2.24}$$

$$t_R(\text{rupture time}) = \frac{\left(\frac{\sigma}{A_d}\right)^{\zeta}}{\phi + 1} \tag{2.25}$$

For some materials, if the damage parameter values are not available in literature, we can obtain them using log-linear Larson–Miller (LM) correlation. From the Larson–Miller fitting, we first obtain a relation between stress as a function of rupture time. Integrating the damage equation, Eq. (2.4) also gives a similar relation,

$$\omega(t) = 1 - \left(1 - \frac{t}{\left(\frac{\sigma}{A}\right)^{-\zeta}\ (1+\phi)^{-1}}\right)^{\frac{1}{1+\phi}} \tag{2.26}$$

which for $\omega = 1$ makes t the rupture time, t_R, Eq. (2.25). Comparing the two rupture time versus stress relations (from LM fitting and damage rate integration) and fixing one of the damage parameters (for example ϕ) we can obtain the values of the remaining damage parameters.

3 Experimental procedure

3.1 General procedure

In this chapter we summarize the method for extracting uniaxial creep parameters from micro indentation creep tests discussed in the previous chapter. Experimental verification of the methodology can be done with undamaged material. The maximum indentation depth for a spherical indenter should be less than the indenter tip radius. For the cylindrical sample, its radius and height should be much larger than the indenter tip radius and the maximum indentation depth, respectively, to avoid any boundary effects. With successful indentation creep experiments (constant depth hold and constant load hold) the uniaxial creep parameters can be extracted as:

- From the load displacement response get the required indentation stress-rate vs. indentation stress data for constant depth hold (CDH) tests, and indentation strain rate vs. indentation stress data for constant load hold (CLH) tests.
- Plot these quantities on a log-log scale and extract the indentation creep exponent and indentation creep coefficient from the slope and intercept.
- The creep exponent obtained from indentation test is the same as that from uniaxial creep test (assuming the sample follows power law creep).
- Using the analysis in the previous study convert the uniaxial creep exponent from the respective CDH or CLH indentation creep test.

Repeat the tests for different hold times, maximum indentation depths, and maximum indent loads to determine their influence on the results. Additionally, perform a few reproducibility tests to estimate the uncertainties associated with the equipment and the material heats.

The indentation equipment needs to be calibrated for the material prior to repeating this analysis with the damaged material. For the calibration study, perform uniaxial creep tests at multiple creep stresses and extract the uniaxial creep parameters (exponent and coefficient) from the steady state creep rates using a power law relation. Alternatively, identify these parameters for undamaged material from the literature. The exponent between the uniaxial and indentation creep tests should be similar. The values of the adjustment factor, κ, mentioned in the previous chapter, required to obtain uniaxial creep coefficient from the indentation creep experiment, can also be fine-tuned from the calibration tests.

Once the equipment is calibrated, implement the following methodology to obtain remaining life of a damaged material:

- Perform the indentation creep (preferably constant depth hold) test on the damaged material.
- Extract the uniaxial creep parameters from the indentation creep test following the methodology discussed earlier.
- The creep exponent should be consistent between the damaged and the undamaged material as it is not history dependent.

- Obtain the current damage in the material from the extracted creep parameters of the damaged material using the indentation test and the uniaxial creep coefficient.

- Determine the current lifetime from the calculated damage using the integral of the damage rate equation.

- The remaining life can then be obtained from the ratio between the current lifetime and rupture time.

This methodology assumes some knowledge of the uniaxial creep parameters of the undamaged material, as well as the damage parameters to calculate the rupture time.

A major assumption of this methodology is the choice of power law creep to describe the material behavior which might be an oversimplification. Additionally, the approach neglects the indentation size effect, i.e., increase in indentation stress and strain with increasing depth. Another challenge is the time required to reach steady state creep, which might require long term tests and might lead to more scatter in the data. The stress exponent in the primary transient regime is higher and can lead to inaccurate results if steady state is not reached. Repeating the tests with different hold times could help control this effect. These theoretical limitations are in addition to experimental challenges. Indentation creep experiments are subject to significant challenges including thermal drift during hold times, ensuring vacuum during indentation to avoid oxidation, and maintaining high temperatures in the indentation chamber.

3.2 Example

The following is an example applying the remaining life assessment approach:

- With a material of known uniaxial creep parameters for an undamaged materials, $A_c = 2 \times 10^{-16}$, and $n_c = 6.0$, perform a constant depth indentation creep experiment at a damaged state. The maximum indentation depth, h_s in Fig. 2.1, for this example is 0.04 mm.

- Generate the indentation load as a function of hold time from the experiment, Fig. 3.1,

- From the indentation load calculate the indentation stress, σ, using,

$$\sigma = \frac{P}{A_{nom}}, \quad \text{with} \tag{3.1}$$

$$A_{nom} = \pi \left(2\, R_{eff}\, 0.04 - 0.04^2\right), \quad \text{and} \tag{3.2}$$

$$\frac{1}{R_{eff}} = \frac{1}{R_{indenter}} + \frac{1}{R_{substrate}} \tag{3.3}$$

where the indenter tip radius, $R_{indenter}$, and sample radius, $R_{substrate}$, are 1 and 4 mm, respectively, R_{eff} is the effective radius, and P is the indentation load shown in Fig. 3.1. Numerically differentiating the indentation stress gives the indentation stress rate, $\dot{\sigma}$.

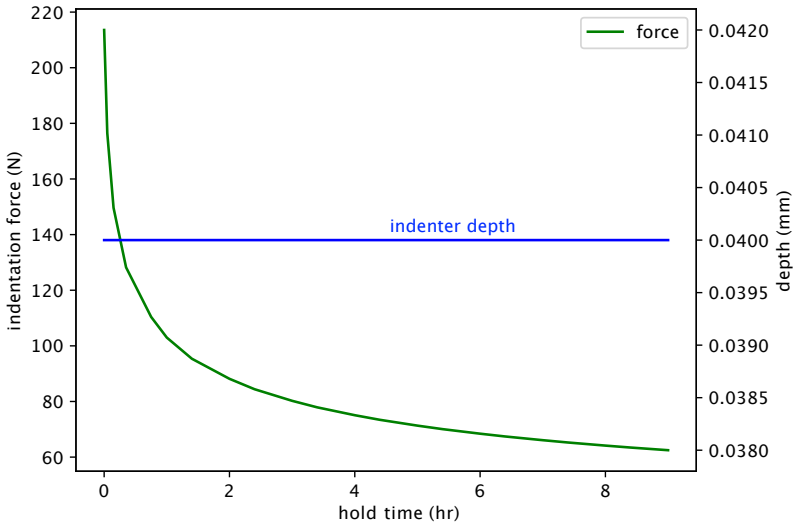

Figure 3.1: Indentation load versus time for a damaged material with creep parameters $n_c = 6.0$ and $A_c = 2 \times 10^{-16}$ for the undamaged material. The maximum indentation depth is 0.04 mm

- Fit the calculated σ and $\dot{\sigma}$ to the following,

$$\frac{\dot{\sigma}}{E_{eff}} = -A\sigma^N, \quad \text{with} \tag{3.4}$$

$$\frac{1}{E_{eff}} = \frac{1-\nu_i^2}{E_{indenter}} + \frac{1-\nu_s^2}{E_{substrate}}, \tag{3.5}$$

  where the Young's modulus and Poisson's ratio of the indenter are $E_{indenter} = 1500$ GPa, $\nu_i = 0.2$, and the substrate $E_{substrate} = 150$ GPa, $\nu_s = 0.31$, respectively. From the fitted data, Fig. 3.2, get the values of the parameters, $N = 6.08$, and $A = 4.15 \times 10^{-15}$.

- From the parameter A calculate the corrected indentation creep coefficient, β using,

$$\beta = \frac{A\,(F\kappa)^N\,c^{2N}}{E_{eff}} \tag{3.6}$$

  where the values of F and c are 2.94 and 1.09 respectively, using the relations provided in Bower et al. [11], and κ is 1.565 based from Table 2.2. The corrected creep coefficient from indentation creep, β, is then 8.76×10^{-16}.

- The current damage, ω, using,

$$\omega = \left(1 - \frac{\beta}{A_c}\right)^{1/N} \tag{3.7}$$

  is then 0.215 with values of A_c, β, and N as 2×10^{-16}, 8.76×10^{-16}, and 6.08, respectively.

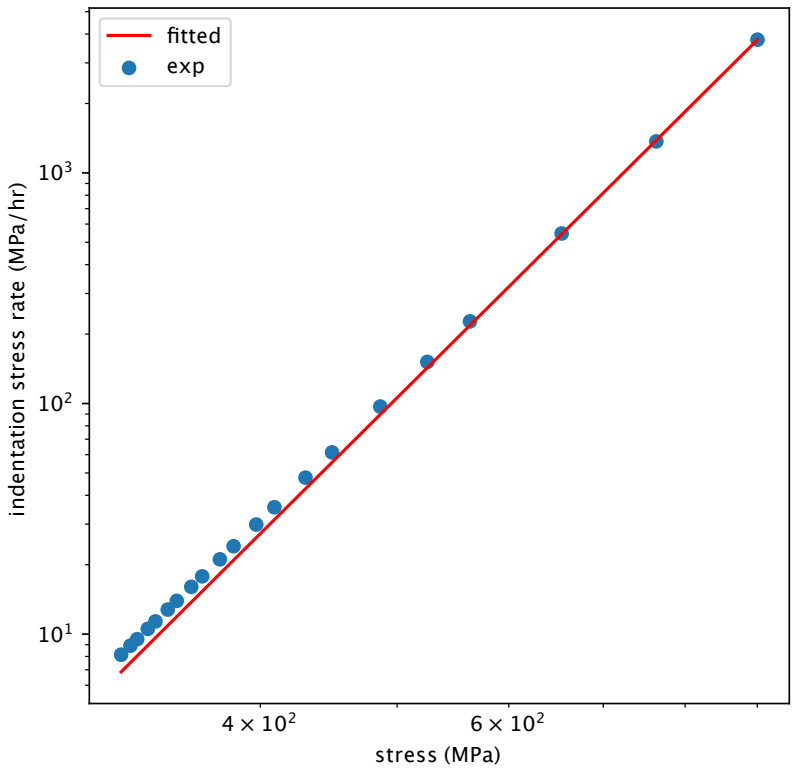

Figure 3.2: Fitted indentation stress rate to stress with a power law.

- Calculate the rupture time,t_R, using the relation (with known damage parameters),

$$t_R = \frac{\left(\frac{\sigma}{A_d}\right)^{\zeta}}{\phi + 1} \tag{3.8}$$

  The damage parameters can be either obtained from literature or using Larson–Miller relation as discussed in the previous chapter. Here, we use $A_d = 1000.0$, $\zeta = 3.5$, and $\phi = 1.5$, and stress (corresponding to the uniaxial creep stress) of 100 MPa resulting in a rupture time of 1265 hours.

- Current used time is calculated using the damage value ($\omega = 0.215$) and integrated damage equation and previously mentioned damage parameters,

$$t = \frac{1 - (1 - \omega)^{\phi+1}}{(\phi + 1)\left(\frac{\sigma}{A_d}\right)^{\zeta}} \tag{3.9}$$

  The calculated use time for a damaged state of 0.215 is 576.1 hours.

- The fraction of remaining life, t_r, is,

$$t_r = 1 - 576.1/1265 = 0.544, \tag{3.10}$$
$$\tag{3.11}$$

  Thus, the given damaged material has 54.4 % life remaining.

We also investigate the sensitivity of κ to the remaining life by repeating the analysis for κ = 1.4 and 1.6. Decreasing the value of κ from 1.565 to 1.4 decreases the used time of the damaged material from 576.1 hours to 355 hours (71.9 % remaining life from 54.4 %), while increasing it to 1.6 increases the used time to 704.8 hours (44.2 % remaining life).

4 Conclusions

This report describes the theory underlying a method for assessing the remaining creep life of a sample of material exposed to unknown service conditions. This approach could be used to assess the remaining life of in situ surveillance test articles placed in future advanced reactors as part of a program designed to ensure adequate component integrity given the relatively unknown impact of the reactor coolant and radiation environment of the mechanical properties of structural materials.

The testing protocol devised here uses microindentation relaxation or creep tests to assess the remaining life of the material given a full characterization of the virgin material properties. The derivation is entirely, at this point, theoretical and based on comparative FEA studies. However, there is a body of literature supporting the basic technique using actual experimental indentation experiments. The approach described here could serve as the nucleus for the test program corresponding to the development of passively-loaded monitoring specimens.

The next immediate step is to validate the results detailed here using actual high temperature indentation testing. The ideal validation test would involve two creep rupture experiments on well-characterized materials from the same heat. One sample would be interrupted before the predicted failure time and the other sample taken to rupture. The interrupted sample could be assessed with the approach described here and the predicted remaining life validated against the ruptured specimen. Similar tests could include environmental effects, given the ability to perform a controlled creep test in representative coolant conditions.

Additional work will be required to integrate the passive monitoring specimen design with the requirements of the indentation testing. This co-design will be particularly important if the surveillance program will replace samples after testing, as the samples will then need to be designed to be accessed by the indenter without destructive prior machining.

Finally, future test programs will need to address cyclic loading and creep-fatigue interaction. The indentation approach described here is adequate only for loading under steady state conditions or for cyclic conditions where fatigue and creep-fatigue damage are negligible.

Acknowledgements

The research was sponsored by the U.S. Department of Energy, under Contract No. DEAC02-06CH11357 with Argonne National Laboratory, managed and operated by UChicago Argonne LLC. Programmatic direction was provided by the Office of Nuclear Reactor Deployment of the Office of Nuclear Energy. The authors gratefully acknowledge the support provided by Sue Lesica, Federal Manager, Advanced Materials, Advanced Reactor Technologies (ART) Program, and Lou Qualls of Oak Ridge National Laboratory, National Technical Director, ART Molten Salt Reactors Campaign.

Bibliography

[1] P Yvon and F Carré. Structural materials challenges for advanced reactor systems. *Journal of Nuclear Materials*, 385(2):217–222, 2009.

[2] KL Murty and I Charit. Structural materials for gen-iv nuclear reactors: Challenges and opportunities. *Journal of Nuclear Materials*, 383(1-2):189–195, 2008.

[3] ASTM E2956-14. Standard Guide for Monitoring the Neutron Exposure of LWR Reactor Pressure Vessels. Standard, ASTM, 2015.

[4] RW Kozar, AW Jaworski, TW Webb, and RW Smith. In situ monitored in-pile creep testing of zirconium alloys. *Journal of Nuclear Materials*, 444(1-3):14–22, 2014.

[5] MC Messner, V-T Phan, RI Jetter, and T-L Sham. Assessment of passively actuated in-situ cyclic surveillance test specimens for advanced non-light water reactors. In *Pressure Vessels and Piping Conference*, volume 51593, page V01BT01A018. American Society of Mechanical Engineers, 2018.

[6] Ted L Anderson and David A Osage. API 579: a comprehensive fitness-for-service guide. *International Journal of Pressure Vessels and Piping*, 77(14-15):953–963, 2000.

[7] Martin Prager. The omega method–an engineering approach to life assessment. *J. Pressure Vessel Technol.*, 122(3):273–280, 2000.

[8] Cody J. Permann, Derek R. Gaston, David Andrš, Robert W. Carlsen, Fande Kong, Alexander D. Lindsay, Jason M. Miller, John W. Peterson, Andrew E. Slaughter, Roy H. Stogner, and Richard C. Martineau. MOOSE: Enabling massively parallel multiphysics simulation. *SoftwareX*, 11:100430, jan 2020. ISSN 23527110. doi:10.1016/j.softx.2020.100430.

[9] F. A. Leckie and D. R. Hayhurst. Constitutive equations for creep rupture. *Acta Metallurgica*, 25(9):1059–1070, 1977. ISSN 00016160. doi:10.1016/0001-6160(77)90135-3.

[10] Ryan S. Ginder, William D. Nix, and George M. Pharr. A simple model for indentation creep. *Journal of the Mechanics and Physics of Solids*, 112:552–562, mar 2018. ISSN 00225096. doi:10.1016/j.jmps.2018.01.001.

[11] A. F. Bower, N. A. Fleck, A. Needleman, and N. Ogbonna. Indentation of a power law creeping solid. *Proceedings - Royal Society of London, A*, 441(1911):97–124, 1993. ISSN 0962-8444. doi:10.1098/rspa.1993.0050.

[12] Caijun Su, Erik G. Herbert, Sangjoon Sohn, James A. LaManna, Warren C. Oliver, and George M. Pharr. Measurement of power-law creep parameters by instrumented indentation methods. *Journal of the Mechanics and Physics of Solids*, 61(2):517–536, feb 2013. ISSN 00225096. doi:10.1016/j.jmps.2012.09.009.

[13] Aritra Chakraborty, Chen Zhang, Shanoob Balachandran, Thomas R. Bieler, and Philip Eisenlohr. Assessment of surface and bulk-dominated methodologies to measure critical resolved shear stresses in hexagonal materials. *Acta Materialia*, 184:241–253, feb 2020. ISSN 13596454. doi:10.1016/j.actamat.2019.11.023.

[14] Aritra Chakraborty and Philip Eisenlohr. Evaluation of an inverse methodology for estimating constitutive parameters in face-centered cubic materials from single crystal indentations. *European Journal of Mechanics, A/Solids*, 66:114–124, nov 2017. ISSN 09977538. doi:10.1016/j.euromechsol.2017.06.012.

[15] In Chul Choi, Byung Gil Yoo, Yong Jae Kim, and Jae Il Jang. Indentation creep revisited, jan 2012. ISSN 08842914.

Applied Materials Division
Argonne National Laboratory
9700 South Cass Avenue, Bldg. 212
Argonne, IL 60439

www.anl.gov